Synthesis, Emission, and Electrochemical Properties of Luminescent Dinuclear Zinc(II) Chalcogenolate Complexes. Dynamic ^{1}H NMR Studies and X-ray Crystal Structure of [(bpy)Zn_2(SC_6H_4-Cl-*p*)(*μ*-SC_6H_4-Cl-*p*)(*μ*-OAc)$_2$]

Vivian Wing-Wah Yam,* Yung-Lin Pui, and Kung-Kai Cheung

Department of Chemistry, The University of Hong Kong, Pokfulam Road, Hong Kong SAR, People's Republic of China

Received June 23, 2000

A series of novel luminescent dinuclear zinc(II) diimine complexes with bridging chalcogenolate ligands have been synthesized, in which the two zinc atoms were found to exist in different coordination environment. The luminescence and electrochemical behavior of these complexes have been studied. These complexes have also been shown to exhibit dynamic fluxional behavior in solution due to an exchange of the bridging and terminal thiolate ligands. The mechanism and kinetics of which have been investigated by variable-temperature ^{1}H NMR studies. The X-ray crystal structure of [(bpy)Zn_2(SC_6H_4-Cl-*p*)(*μ*-SC_6H_4-Cl-*p*)(*μ*-OAc)$_2$] has also been determined.

Introduction

Zinc(II) thiolate complexes have been used as models for thiolate metalloproteins, in which zinc centers are frequently coordinated through histidines and the sulfur-containing cysteine.[1] Moreover, zinc complexes with S_4, S_3N, or S_2N_2 ligand cores are of interest as structural models of the immediate ligand environment of zinc in DNA-binding proteins and certain zinc-containing enzymes.[2] In view of this, an understanding of its basic coordination properties is necessary. Although there are numerous reports on zinc(II) thiolate systems,[3] most of the studies were limited to those of structural studies, in which the zinc atom generally is found to assume a tetrahedral geometry with the corresponding studies on the less common five-coordinate zinc(II) complexes[4,5] being relatively less explored. Coordination geometries other than that of four are interesting in view of the possibility of zinc to exist as penta-, tri-, and perhaps even hexa-coordinated structures in the functional states of the biological systems. Intrigued by the recent reports on the observation of colored complexes of these closed-shell metal centers, particularly those of zinc(II) coordinated to diimine and thiolate ligands and the luminescence properties of a number of these complexes,[5] efforts have been made to explore the thiolate chemistry and luminescence properties of zinc(II) complexes. Since most of the luminescence studies reported so far are confined to the mononuclear zinc(II) diimine dithiolate systems[5] with only a few reports on the polynuclear anionic zinc thiolates,[6] it would be interesting to design dinuclear analogues by utilizing the chalcogenolate as possible bridging ligands.

In this report, a series of novel dinuclear zinc(II) chalcogenolate complexes have been synthesized and shown to exhibit interesting luminescence and electrochemical properties. These complexes have been shown to exhibit dynamic fluxional behavior in solution due to an exchange of the bridging and terminal thiolate ligands; the mechanism of which has been investigated by variable-temperature ^{1}H NMR studies. The X-ray crystal structure of one of the complexes has also been determined.

Experimental Section

Materials and Reagents. Thiophenol and 4-fluorothiophenol were obtained from Aldrich Chemical Company. Zinc acetate dihydrate, 4-methoxythiophenol, 4-chlorothiophenol, and 2,2′-bipyridine were obtained from Lancaster Synthesis Ltd. 4,4′-Di-*tert*-butyl-2,2′-bipyridine (^{t}Bu$_2$bpy) was prepared by the modification of a literature procedure.[7] Tetrabutylammonium hexafluorophosphate (^{n}Bu$_4$NPF$_6$) (Aldrich, 98%)

(1) (a) Klug, A.; Rhodes, D. *Trends Biochem. Sci*. **1987**, *12*, 464. (b) Berg, J. M. *Prog. Inorg. Chem*. **1989**, *37*, 143. (c) Vallee, B. L.; Auld, D. S. *Biochemistry* **1990**, *29*, 5647. (d) Vallee, B. L.; Coleman, J. E. *Proc. Natl. Acad. Sci., U. S. A.* **1991**, *88*, 999. (e) Coleman, J. E. *Annu. Rev. Biochem*. **1992**, *61*, 897. (f) Vallee, B. L.; Auld, D. S. *Biochemistry* **1993**, *32*, 6493.

(2) (a) Hough, E.; Hansen, L. K.; Birkness, B.; Jynge, K.; Hansen, S.; Hordvik, A.; Little, C.; Dodson, E.; Derewenda, Z. *Nature (London)* **1989**, *338*, 357. (b) Alsfasser, R.; Powell, A. K.; Vahrenkamp, H. *Angew. Chem., Int. Ed. Engl*. **1990**, *29*, 898. (c) Uhlenbrock, S.; Krebs, B. *Angew. Chem., Int. Ed. Engl*. **1992**, *31*, 1647. (d) Hansen, S.; Hansen, L. K.; Hough, E. *J. Mol. Biol.* **1993**, *231*, 870.

(3) (a) Dance, I. G. *J. Am. Chem. Soc.* **1980**, *102*, 3445. (b) Choy, A.; Craig, D.; Dance, I. G.; Scudder, M. *J. Chem. Soc., Chem. Commun.* **1982**, 1246. (c) Dance, I. G.; Choy, A.; Scudder, M. L. *J. Am. Chem. Soc.* **1984**, *106*, 6285. (d) Watson, A. D.; Rao, C. P.; Dorfman, J. R.; Holm, R. H. *Inorg. Chem.* **1985**, *24*, 2820. (e) Abrahams, I. L.; Garner, C. D. *J. Chem. Soc., Dalton. Trans.* **1987**, 1577. (f) Vittal, J. J.; Dean, P. A. W.; Payne, N. C. *Inorg. Chem.* **1987**, *26*, 1683. (g) Ueyama, N.; Sugawara, T.; Sasaki, K.; Nakamura, A.; Yamashita, S.; Wakatsuki, Y.; Yamazaki, H.; Yasuoka, N. *Inorg. Chem.* **1988**, *27*, 741. (h) Dean, P. A. W.; Vittal, J. J.; Payne, N. C. *Can. J. Chem.* **1992**, *70*, 792. (i) Melnik, M. *J. Coord. Chem.* **1995**, *35*, 179. (j) Anjali, K. S.; Sampanthar, J. T.; Vittal, J. J. *Inorg. Chim. Acta* **1999**, *295*, 9.

(4) (a) Lee, G. S. H.; Craig, D. C.; Ma, I.; Scudder, M. L.; Bailey T. D.; Dance, I. G. *J. Am. Chem. Soc.* **1988**, *110*, 4863. (b) Zhang, C.; Chadha, R.; Reddy H. K.; Schrauzer, G. N. *Inorg. Chem.* **1991**, *30*, 3865. (c) Gronlund, P. J.; Wacholtz, W. F.; Mague, J. T. *Acta Crystallogr.* **1995**, *C51*, 1540. (d) Uhlenbrock, S.; Wegner, R.; Krebs, B. *J. Chem. Soc., Dalton Trans.* **1996**, 3731.

(5) (a) Crosby, G. A.; Highland, R. G.; Truesdell, K. A. *Coord. Chem. Rev.* **1985**, *64*, 41. (b) Truesdell, K. A.; Crosby, G. A. *J. Am. Chem. Soc.* **1985**, *107*, 1781. (c) Highland, R. G.; Brummer, J. G.; Crosby, G. A. *J. Phys. Chem.* **1986**, *90*, 1593. (d) Jordan, K. J.; Wacholtz, W. F.; Crosby, G. A. *Inorg. Chem.* **1991**, *30*, 4588.

(6) (a) Türk, T.; Resch, U.; Fox, M. A.; Vogler, A. *Inorg. Chem.* **1992**, *31*, 1854. (b) Türk, T.; Vogler, A.; Fox, M. A. *Adv. Chem. Ser.* **1993**, 233.

(7) (a) Sasse, W. H. F.; Whittle, C. P. *J. Chem. Soc.* **1961**, 1347. (b) Sasse, W. H. F. *Org. Syn.* **1973**, *V*, 102.

10.1021/ic000688g CCC: $19.00
Published on Web 11/15/2000

was purified by recrystallization with ethanol three times before use. Dichloromethane was purified using standard procedures before use.[8] All other reagents were of analytical grade and were used as received.

[(bpy)$Zn_2(SC_6H_5)(\mu$-$SC_6H_5)(\mu$-OAc$)_2$] (1). To a stirred solution of zinc acetate dihydrate (100 mg, 0.46 mmol) in methanol (5 mL) was added a solution of 2,2′-bipyridine (72 mg, 0.46 mmol) in methanol (5 mL). The resultant solution was stirred for 30 min under a nitrogen atmosphere. Thiophenol (50 mg, 0.46 mmol) dissolved in dichloromethane (10 mL) was then added to the reaction mixture dropwise with stirring to produce an immediate color change from a colorless to yellow solution. The mixture was stirred overnight under a nitrogen atmosphere. After evaporation of the solvent, the residue was dissolved in dichloromethane, and diffusion of diethyl ether vapor into its concentrated solution gave **1** as white crystals. Yield: 88 mg (62%). ^{1}H NMR (300 MHz, $CDCl_3$, 298 K, relative to Me_4Si): δ 2.05 (s, 6H, OAc), 6.90 (m, 6H, aryl H ortho to S), 7.30 (m, 4H, aryl H meta to S), 7.45 (t, 2H, $J = 12.6$ Hz, bpy H's), 8.05 (t, 2H, $J = 16.6$ Hz, bpy H's), 8.15 (d, 2H, $J = 7.8$ Hz, bpy H's), 8.60 (unresolved d, 2H, bpy H's). Anal. Calcd for $C_{26}H_{24}N_2O_4S_2Zn_2$: C, 50.10; H, 3.88; N, 4.49. Found: C, 49.99; H, 3.89; N, 4.40.

[(bpy)$Zn_2(SC_6H_4$-F-*p*$)(\mu$-SC_6H_4-F-*p*$)(\mu$-OAc$)_2$] (2). The procedure was similar to that described for the preparation of **1**, except 4-fluorothiophenol (59 mg, 0.46 mmol) was used in place of thiophenol to give white crystals of **2**. Yield: 90 mg (59%). ^{1}H NMR (300 MHz, $CDCl_3$, 298 K, relative to Me_4Si): δ 2.05 (s, 6H, OAc), 6.60 (d, 4H, $J = 8.4$ Hz, aryl H ortho to S), 7.20 (d, 4H, $J = 8.2$ Hz, aryl H meta to S), 7.50 (t, 2H, $J = 13.3$ Hz, bpy H's), 8.05 (t, 2H, $J = 15.4$ Hz, bpy H's), 8.15 (d, 2H, $J = 7.9$ Hz, bpy H's), 8.60 (unresolved d, 2H, bpy H's). Anal. Calcd for $C_{26}H_{22}F_2N_2O_4S_2Zn_2$: C, 47.36; H, 3.36; N, 4.25. Found: C, 47.37; H, 3.37; N, 4.27.

[(bpy)$Zn_2(SC_6H_4$-Cl-*p*$)(\mu$-SC_6H_4-Cl-*p*$)(\mu$-OAc$)_2$] (3). The procedure was similar to that described for the preparation of **1**, except 4-chlorothiophenol (67 mg, 0.46 mmol) was used in place of thiophenol to give white crystals of **3**. Yield: 80 mg (51%). ^{1}H NMR (300 MHz, $CDCl_3$, 298 K, relative to Me_4Si): δ 2.05 (s, 6H, OAc), 6.85 (d, 4H, $J = 8.1$ Hz, aryl H ortho to S), 7.20 (d, 4H, $J = 8.0$ Hz, aryl H meta to S), 7.55 (t, 2H, $J = 12.7$ Hz, bpy H's), 8.10 (t, 2H, $J = 17.1$ Hz, bpy H's), 8.17 (d, 2H, $J = 8.0$ Hz, bpy H's), 8.62 (unresolved d, 2H, bpy H's). Anal. Calcd for $C_{26}H_{22}Cl_2N_2O_4S_2Zn_2$: C, 45.11; H, 3.20; N, 4.05. Found: C, 44.84; H, 3.28; N, 4.05.

[(bpy)$Zn_2(SC_6H_4$-OCH_3-*p*$)(\mu$-SC_6H_4-OCH_3-*p*$)(\mu$-OAc$)_2$] (4). The procedure was similar to that described for the preparation of **1**, except 4-methoxythiophenol (64 mg, 0.46 mmol) was used in place of thiophenol to give pale yellow crystals of **4**. Yield: 86 mg (55%). ^{1}H NMR (300 MHz, $CDCl_3$, 298 K, relative to Me_4Si): δ 2.05 (s, 6H, OAc), 3.65 (s, 6H, OCH_3), 6.50 (d, 4H, $J = 6.4$ Hz, aryl H ortho to S), 7.18 (d, 4H, $J = 6.1$ Hz, aryl H meta to S), 7.50 (t, 2H, $J = 12.5$ Hz, bpy H's), 8.05 (t, 2H, $J = 16.9$ Hz, bpy H's), 8.15 (d, 2H, $J = 7.7$ Hz, bpy H's), 8.65 (unresolved d, 2H, bpy H's). Anal. Calcd for $C_{28}H_{28}N_2O_6S_2Zn_2$: C, 49.21; H, 4.13; N, 4.10. Found: C, 48.86; H, 4.12; N, 3.84.

[(^{t}Bu$_2$bpy)$Zn_2(SC_6H_5)(\mu$-$SC_6H_5)(\mu$-OAc$)_2$] (5). The procedure was similar to that described for the preparation of **1**, except 4,4′-di-*tert*-butyl-2,2′-bipyridine[7] (125 mg, 0.47 mmol) was used in place of 2,2′-bipyridine to give white crystals of **5**. Yield: 74 mg (44%). ^{1}H NMR (300 MHz, $CDCl_3$, 298 K, relative to Me_4Si): δ 1.40 (s, 18H, ^{t}Bu), 2.03 (s, 6H, OAc), 6.90 (m, 6H, aryl H ortho to S), 7.25 (m, 4H, aryl H meta to S), 7.40 (m, 2H, bpy H's), 8.00 (m, 2H, bpy H's), 8.50 (m, 2H, bpy H's). Anal. Calcd for $C_{34}H_{40}N_2O_4S_2Zn_2\cdot H_2O$: C, 54.19; H, 5.62; N, 3.72. Found: C, 54.53; H, 5.49; N, 3.58.

Physical Measurements and Instrumentation. ^{1}H NMR spectra were recorded on a Bruker DPX-300 FT-NMR spectrometer (300 MHz) at 298 K, and chemical shifts are reported relative to Me_4Si. Variable-temperature one-dimensional ^{1}H NMR spectra in $CDCl_3$ and two-dimensional COSY and EXSY in CD_2Cl_2 at 223 K were recorded on a Bruker DRX-500 FT-NMR spectrometer (500 MHz). Elemental analyses of the new complexes were performed on a Carlo Erba 1106 elemental analyzer at the Institute of Chemistry, Chinese Academy of Sciences.

UV/vis spectra were obtained on a Hewlett-Packard 8452A diode array spectrophotometer, and steady-state excitation and emission spectra on a Spex Fluorolog 111 spectrofluorimeter. For solution emission and excitation spectra, samples were degassed on a high-vacuum line (limiting pressure $< 10^{-3}$ Torr) in a two compartment cell consisting of a 10-mL Pyrex bulb equipped with a sidearm 1-cm fluorescence cuvettte and sealed from the atmosphere by a Rotaflo HP6/6 quick-release Teflon stopper. Solutions were rigorously degassed with no fewer than four freeze−pump−thaw cycles. The concentration of the solutions are in the range of 10^{-4} to 10^{-5} M. Solid-state emission and excitation spectra at room temperature were recorded with ground solid samples loaded in a quartz tube inside a quartz-walled Dewar flask. Solid-state spectra at low temperature (77 K) were similarly recorded with liquid nitrogen inside the optical Dewar flask.

Cyclic voltammetric measurements were performed by using a CH Instruments, Inc., CHI 620 electrochemical analyzer interfaced to an IBM-compatible PC. The electrolytic cell used was a conventional two-compartment cell. The salt bridge of the reference electrode was separated from the working electrode compartment by a Vycor glass bridge. A $Ag/AgNO_3$ (0.1 mol dm^{-3} in CH_2Cl_2) reference electrode was used. The ferrocenium−ferrocene couple ($FeCp_2^{+/0}$) was used as the internal reference in the electrochemical measurements.[9a] The working electrode was a glassy carbon (Atomergic Chemetals V25) electrode with a platinum foil acting as the counter electrode. Treatment of the electrode surfaces was as reported previously.[9b]

Crystal Structure Determination. Crystal data for [(bpy)Zn_2-(SC_6H_4−Cl-*p*)(μ-SC_6H_4−Cl-*p*)(μ-OAc)$_2$] (**3**): [$C_{26}H_{22}Cl_2N_2O_4S_2Zn_2$]; fw = 692.26, triclinic, space group $P\bar{1}$ (No. 2), $a = 7.997(1)$ Å, $b = 10.297(2)$ Å, $c = 18.550(2)$ Å, $\alpha = 105.46(1)°$, $\beta = 93.23(1)°$, $\gamma = 97.25(1)°$, $V = 1454.0(9)$ Å^3, $Z = 2$, $D_c = 1.581$ g cm^{-3}, μ(Mo Kα) = 20.11 cm^{-1}, $F(000) = 700$, T = 301 K. A colorless crystal of dimensions 0.35 × 0.20 × 0.05 mm mounted on a glass fiber was used for data collection at 28 °C on a Rigaku AFC7R diffractometer with graphite-monochromated Mo Kα radiation ($\lambda = 0.71073$ Å) using $\omega-2\theta$ scans with ω-scan angle $(0.73 + 0.35 \tan\theta)°$ at a scan speed of 8.0 deg min^{-1} (up to 6 scans for reflection with $I < 15\sigma(I)$). Unit-cell dimensions were determined on the basis of the setting angles of 25 reflections in the 2θ range of 29.3 to 34.2°. Intensity data (in the range of $2\theta_{max} = 50°$; h −9 to 9; k 0 to 12; l −22 to 21 and three standard reflections measured after every 300 reflections showed decay of 1.25%) were corrected for decay and for Lorentz and polarization effects, and empirical absorption corrections based on the ψ-scan of five strong reflections (minimum and maximum transmission factors 0.625 and 1.000); 5459 reflections were measured, of which 5144 were unique and $R_{int} = 0.016$, and 3635 reflections with $I > 3\sigma(I)$ were considered observed and used in the structural analysis. The space group was determined based on a statistical analysis of intensity distribution and the successful refinement of the structure solved by direct methods (SIR92)[10a] and expanded by Fourier method and refined by full-matrix least-squares using the software package TeXsan[10b] on a Silicon Graphics Indy computer. One crystallographic asymmetric unit consists of one molecule. In the least-squares refinement, all 38 non-H atoms were refined anisotropically and 22 H atoms at calculated positions with thermal parameters equal to 1.3 times that of the attached C atoms were not refined. Convergence for 343 variable parameters by least-squares refinement on F with $w = 4F_o^2/\sigma^2(F_o^2)$, where $\sigma^2(F_o^2) = [\sigma^2(I) + (0.030F_o^2)^2]$ for 3635 reflections with $I > 3\sigma(I)$ was reached at $R = 0.033$ and wR = 0.046 with a goodness-of-fit of 1.68; $(\Delta/\sigma)_{max} = 0.05$. The final difference Fourier map was featureless, with maximum positive and negative peaks of 0.43 and 0.32 e Å^{-3}, respectively.

(8) Perrin, D. D.; Armarego, W. L. F. *Purification of Laboratory Chemicals*, 3rd ed.; Pergamon Press: New York, 1988.

(9) (a) Gagne, R. R.; Koval, C. A.; Lisensky, G. C. *Inorg. Chem.* **1980**, *19*, 2854. (b) Che, C. M.; Wong, K. Y.; Anson, F. C. *J. Electroanal. Chem., Interfacial Electrochem.* **1987**, *226*, 221.

(10) (a) Altomare, A.; Cascarano, M.; Giacovazzo, C.; Guagliardi, A.; Burla, M. C.; Polidori, G.; Camalli, M. *J. Appl. Crystallogr.* **1994**, *27*, 435. (b) *TeXsan*: Crystal Structure Analysis Package, Molecular Structure Corp., 1985 and 1992.

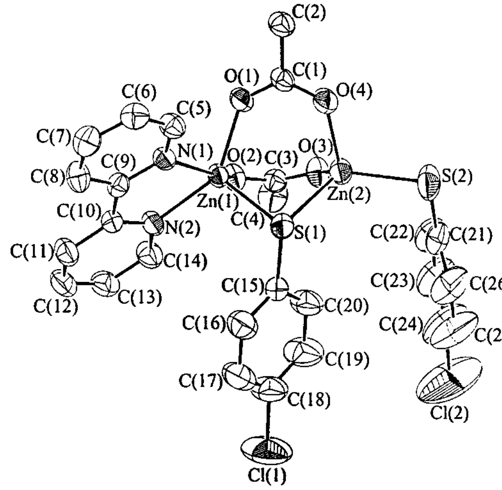

Figure 1. Perspective drawing of **3** with the atomic numbering scheme. Hydrogen atoms have been omitted for clarity. Thermal ellipsoids are shown at the 40% probability level.

Table 1. Selected Geometric Data for **3**

Bond Lengths (Å)			
Zn(1)−S(1)	2.347(1)	Zn(1)−O(1)	2.047(3)
Zn(1)−O(2)	2.039(2)	Zn(1)−N(1)	2.153(3)
Zn(1)−N(12)	2.121(3)	Zn(2)−S(1)	2.379(1)
Zn(2)−S(2)	2.254(1)	Zn(2)−O(3)	1.976(3)
Zn(2)−O(4)	1.982(3)		
Bond Angles (deg)			
S(1)−Zn(1)−O(1)	104.21(8)	S(1)−Zn(1)−O(2)	103.40(8)
S(1)−Zn(1)−N(1)	106.60(8)	S(1)−Zn(1)−N(2)	111.37(9)
O(1)−Zn(1)−O(2)	94.4(1)	O(1)−Zn(1)−N(1)	85.3(1)
O(1)−Zn(1)−N(2)	143.3(1)	N(1)−Zn(1)−N(2)	76.6(1)
S(1)−Zn(2)−S(2)	121.79(5)	S(1)−Zn(2)−O(3)	106.21(8)
S(1)−Zn(2)−O(4)	102.33(9)	S(2)−Zn(2)−O(3)	111.62(9)
S(2)−Zn(2)−O(4)	106.26(9)	O(3)−Zn(2)−O(4)	107.5(1)
Zn(1)−S(1)−Zn(2)	86.97(4)	Zn(1)−S(1)−C(15)	103.9(1)
Zn(2)−S(1)−C(15)	109.5(1)	Zn(2)−S(2)−C(21)	100.0(2)

Results and Discussion

Crystal Structure Determination. All of the complexes were characterized by ^{1}H NMR spectroscopy and gave satisfactory elemental analyses. Single crystals of **3** were obtained by vapor diffusion of diethyl ether into a concentrated dichloromethane solution of the complex. One of the zinc centers adopts a distorted tetrahedral geometry with a S(1)−Zn(2)−S(2) angle of 121.79(5)° while the other adopts a distorted square pyramidal geometry with a S(1)−Zn(1)−N(1) angle of 106.60(8)°. The two metal centers are linked together by a bridging thiolate ligand and two bridging acetates, with a Zn(1)−S(1)−Zn(2) angle of 86.97(4)°. The Zn−S(1) and Zn(2)−S(2) bond distances with the bridging and terminal thiolate ligands are 2.363(1) Å (average) and 2.254(1) Å, respectively, which are comparable to those found in other related systems.[3d,e,j,5d,11] The perspective drawing of **3** with atomic numbering is depicted in Figure 1. Selected bond distances and angles are summarized in Table 1.

Electronic Absorption and Emission Properties. The electronic absorption spectra of complexes **1**−**5** show low-energy absorption shoulders at ca. 340−380 nm and higher energy absorptions at ca. 240−310 nm (Table 2). The latter are assigned as intraligand (IL) transitions of the diimines and chalcogenolates since the free ligands also absorb at similar energy. The low-energy absorption shoulders at 340−380 nm

(11) Halvorsen, K.; Crosby, G. A.; Wacholtz, W. F. *Inorg. Chim. Acta* **1995**, *228*, 81.

Table 2. Electronic Absorption and Emission Data for Complexes **1**−**5**

complex	medium (*T*/K)	λ_{abs}/nm (ϵ/dm^3 mol^{-1} cm^{-1})	λ_{em}/nm[a]
1	solid (298)		510
	solid (77)		525
	glass (77)[b]		530
	CH_2Cl_2 (298)	243 (24 350), 298 (17 810), 308 (17 530), 360sh (280)	
	MeOH (298)	250 (32 540), 297 (16 220), 307 (15 220), 355sh (320)	
2	solid (298)		504
	solid (77)		528
	glass (77)[b]		520
	CH_2Cl_2 (298)	241 (26 140), 298 (16 850), 309 (16 160), 358sh (190)	
	MeOH (298)	258 (27 300), 297 (15 960), 307 (15 010), 356sh (260)	
3	solid (298)		537
	solid (77)		527
	glass (77)[b]		514
	CH_2Cl_2 (298)	250 (28 480), 299 (18 800), 309 (17 930), 352sh (310)	
	MeOH (298)	256 (27 700), 296 (18 310), 307 (16 600), 354sh (240)	
4	solid (298)		555
	solid (77)		544
	glass (77)[b]		540
	CH_2Cl_2 (298)	248 (41 700), 298 (21 550), 308 (20 460), 370sh (310)	
	MeOH (298)	250 (32 410), 298 (19 260), 307 (17 840), 376sh (210)	
5	solid (298)		504
	solid (77)		510
	glass (77)[b]		508
	CH_2Cl_2 (298)	243 (27 150), 298 (15 730), 308 (15 750), 345sh (350)	
	MeOH (298)	250 (30 130), 297 (13 440), 307 (11 300), 350sh (300)	

[a] Excitation wavelength at 350 nm. [b] EtOH: MeOH = 4:1 (v/v).

in dichloromethane and methanol were found to show a slight energy dependence on the nature of the chalcogenolate and the diimine ligands. The low energy absorption shoulder for **1** was found to occur at lower energy compared to that of **5** but at higher energy than that of **4**. Such an energy trend is suggestive of a ligand-to-ligand charge-transfer LLCT [$p_\pi(SR^-) \rightarrow \pi^*(N-N)$] transition assignment, which is in accordance with the higher π^* orbital energy of ^{t}Bu$_2$bpy than bpy and the greater electron-richness of 4-methoxythiophenolate than thiophenolate. Similar findings have also been observed in other related systems.[5]

Upon excitation at $\lambda = 350$ nm, complexes **1**−**5** are found to be luminescent with emission maxima at ca. 500−550 nm both in the solid state at room temperature and 77 K, and in 77 K glass, but they are nonemissive in degassed acetonitrile and methanol solutions. The photophysical data are summarized in Table 2. The emission energies are found to depend on the nature of both the chalcogenolate and the diimine ligands. The emission energies in 77 K glass follow the order: [(bpy)Zn$_2$(SC$_6$H$_4$-OCH$_3$-*p*)(μ-SC$_6$H$_4$-OCH$_3$-*p*)(μ-OAc)$_2$] (**4**) (540 nm) < [(bpy)Zn$_2$(SC$_6$H$_5$)(μ-SC$_6$H$_5$)(μ-OAc)$_2$] (**1**) (530 nm) < [(bpy)Zn$_2$(SC$_6$H$_4$-F-*p*)(μ-SC$_6$H$_4$-F-*p*)(μ-OAc)$_2$] (**2**) (520 nm) < [(bpy)Zn$_2$(SC$_6$H$_4$-Cl-*p*)(μ-SC$_6$H$_4$-Cl-*p*)(μ-OAc)$_2$] (**3**) (514 nm). On the basis of purely inductive effects alone, the electron-donating ability of the thiophenolate ligands is expected to occur in the order SC$_6$H$_4$-OCH$_3$-*p* > SC$_6$H$_5$ > SC$_6$H$_4$-Cl-*p* > SC$_6$H$_4$-F-*p*. Therefore the LLCT emission energies would be expected to show an energy trend in the order **4** < **1** < **3** $\leqslant$ **2** with the same bipyridine ligand, which is more or less in line with the

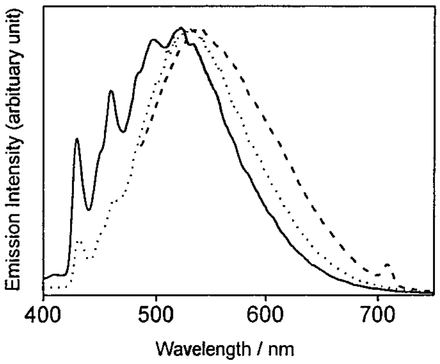

Figure 2. Emission spectra of **1** (···), **3** (—) and **4** (- - -) in EtOH/MeOH (4:1 v/v) glass at 77 K. Excitation wavelength at 350 nm. [**1**], [**3**], and [**4**] = 1 × 10^{-3} M.

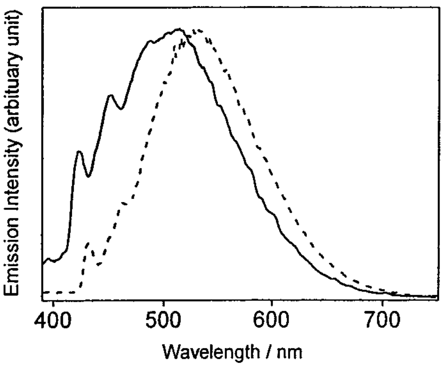

Figure 3. Emission spectra of **1** (- - -) and **5** (—) in EtOH/MeOH (4:1 v/v) glass at 77 K. Excitation wavelength at 350 nm. [**1**] and [**5**] = 1 × 10^{-3} M.

experimental findings. The only anomaly is seen for **2** and **3** in which the fluoro-substituted **2** emits at lower energy than its chloro analogue **3**. This may be rationalized by the fact that resonance effect of lone pair electron donation from the F atom to the 3d orbitals of sulfur could be more important than its negative inductive effect. For the same chalcogenolate ligand, the lower emission energies for $[(bpy)Zn_2(SC_6H_5)(\mu\text{-}SC_6H_5)(\mu\text{-}OAc)_2]$ (**1**) than that of $[(^tBu_2bpy)Zn_2(SC_6H_5)(\mu\text{-}SC_6H_5)(\mu\text{-}OAc)_2]$ (**5**) is again in line with the assignment of an LLCT emission origin since a higher π^* orbital energy is expected for ^{t}Bu$_2$bpy than bpy. The emission spectra of complexes **1**, **3**, and **4** in EtOH/MeOH (4:1 v/v) glass at 77 K are shown in Figure 2. Figure 3 shows the emission spectra of complexes **1** and **5** in 77 K glass. The observation of vibronic structures on the blue side of the emission band with vibrational progressional spacings of ca. 1570 cm^{-1} in 77 K glass is attributed to the mixing into the broad featureless LLCT emission of a high-energy intraligand IL (diimine) emission, which becomes prominent in 77 K glass. The lack of a trend in the solid-state emission energies, which may result from site heterogeneity commonly observed in the solid states, is understandable.

Dynamic ^{1}H NMR Studies. The ^{1}H NMR spectra of complexes **1**−**5** at 298 K show very complicated pattern, with the aromatic protons on the thiophenolate ligands showing not a simple doublet of doublets (AA′XX′) pattern that is typical of 1,4-disubstituted benzenes. Instead four sets of the thiophenolate protons were observed, suggestive of a fluxional behavior of the system. To provide further insight into such fluxional behavior, a variable-temperature ^{1}H NMR study on $[(bpy)Zn_2(SC_6H_4\text{-}Cl\text{-}p)(\mu\text{-}SC_6H_4\text{-}Cl\text{-}p)(\mu\text{-}OAc)_2]$ (**3**) in $CDCl_3$ in the temperature range of 223−313 K was undertaken. The spectra recorded at low temperatures indicated that the two thiophenolate ligands were inequivalent and were in slow exchange with each other. At higher temperature in $CDCl_3$, the two thiophenolate ligands, the terminal and the bridging at δ 6.85 and 7.20, became equivalent on the ^{1}H NMR time scale, possibly as a result of their increased rate of interconversion. Therefore, only two sets of thiophenolate protons, in the range of δ 6.85 to 7.20 ppm, were observed at 313 K in the ^{1}H NMR spectrum as shown in Figure 4. However, these protons appeared as broad signals as the temperature is lowered as a result of the slow exchange of these two thiophenolate ligands when the complex was frozen down. At 223 K, four sets of thiophenolate signals, δ 6.81, 6.90, 7.02, and 7.50 ppm, were observed in the region, indicating that the exchange of the bridging and the terminal thiophenolate ligands was slow to frozen. Using DNMR line shape simulation program,[12a] the exchange rate constants (k) at different temperature were determined. The $\Delta G^\ddagger$ value for the fluxional process of **3** in $CDCl_3$ obtained from the linear plot of ln k/T versus $1/T$ according to the Eyring equation[12b−c] was found to be ca. 24.4 ± 0.5 kJ mol^{-1}. It is likely to be ascribed to a terminal-to-bridging thiophenolate exchange process. An alternative possible mechanism involves the cleavage of the Zn−$SR_{(bridging)}$ bond at high temperature to give two four-coordinate Zn environments. However, in view of the small activation barrier obtained and the close resemblance of the activation barrier to that observed for bridging-to-terminal thiolate exchange processes in related systems,[13] together with the large amount of energy required for a Zn−S cleavage process (bond energy 37.5 kcalmol^{-1}),[14] the possibility of such a Zn−S bond cleavage mechanism is less likely.

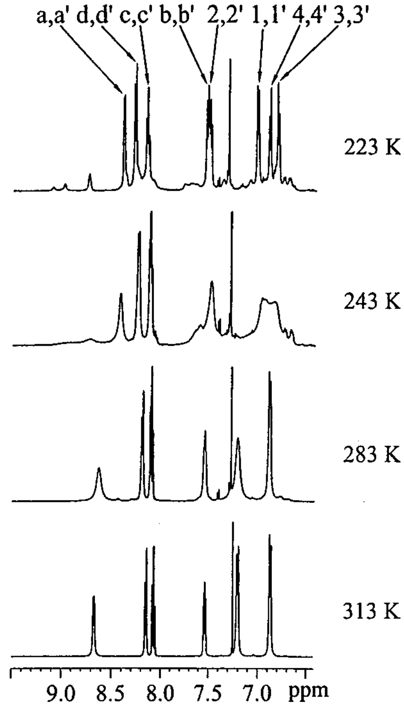

Figure 4. Variable-temperature ^{1}H NMR spectra of **3** in $CDCl_3$.

At the same time, it was interesting to note that, apart from the major species, minor species also occurred when the

(12) (a) DNMR lineform simulation, http://iris.chem.uni-potsdam.de/cgi-bin/perl_prog/lineform.pg. (b) Oki, M. *Application of Dynamic NMR Spectroscopy to Organic Chemistry*; VCH: Deerfield Beach, FL, 1985. (c) Friebolin, H. *Basic One- and Two-Dimensional NMR Spectroscopy*; VCH: Germany, 1991; p 271.

(13) Bochmann, M.; Bwembya, G.; Grinter, R.; Lu, J.; Webb, K. J.; Williamson, D. J. *Inorg. Chem.* **1993**, *32*, 532.

(14) Quartararo, J.; Mignard, S.; Kasztelan, S. *J. Catal.* **2000**, *192*, 307.

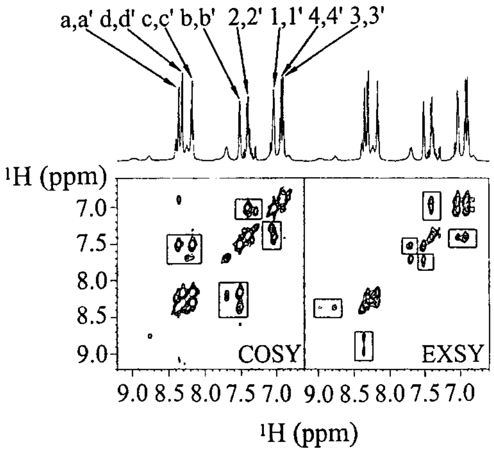

Figure 5. Two-dimensional ^{1}H NMR spectra of **3** in CD_2Cl_2 at 223 K with the normal ^{1}H NMR on top of the spectra. The boxes in COSY highlighted the cross-peaks of vicinal aryl protons within the same species. The cross-peaks inside the boxes in EXSY indicated the exchange of various different conformations of **3** in solution at low temperature (the major and the minor species).

Scheme 1

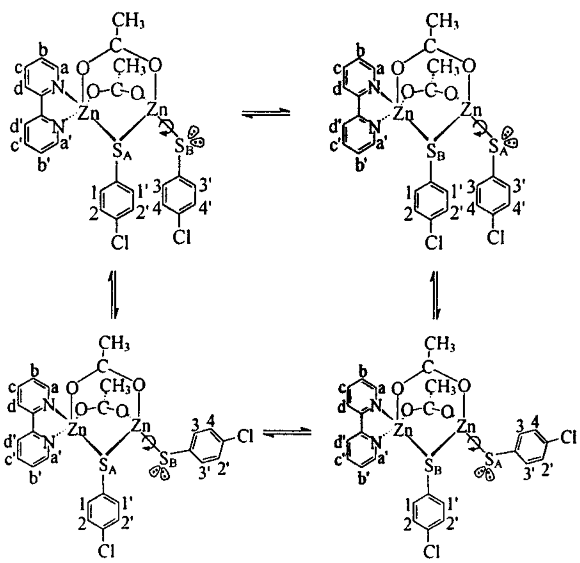

Table 3. Electrochemical Data for Complexes **1**−**5** in Dichloromethane (0.1 mol dm^{-3} $^{n}Bu_4NPF_6$)

complex	oxidation[a,b] E_{pa}/V vs SCE	reduction[a,c] $E_{1/2}$/V vs SCE
1	+1.67, +1.92	−1.52
2	+1.30, +1.64	−1.53
3	+1.66, +1.85	−1.52
4	+1.44, +1.73	−1.55
5	+1.72, +1.99	−1.62

[a] Glassy carbon electrode; ΔE_p of Fc^{+}/Fc ranges from 75 to 80 mV; scan rate, 100 mVs^{-1}. [b] E_{pa} refers to the anodic peak potential of the irreversible oxidation wave. [c] $E_{1/2} = (E_{pa} + E_{pc})/2$ where E_{pa} and E_{pc} are the anodic and cathodic peak potentials of the quasi-reversible reduction couple, respectively.

temperature was lowered. These sets of thiophenolate and bipyridyl protons in the minor species probably are a result of the inability of the lone pairs on the sulfur atoms to flip freely[15] due to a restricted rotation about the Zn−S bond at low temperatures[13] and, therefore, resulted in various conformations, each experiencing a new environment of its own. The acetate proton signals also became broad as the temperature is lowered, most probably attributed to the different environments experienced by these protons when the complex was frozen. On the contrary, the acetate protons appeared as a sharp singlet at 313 K.

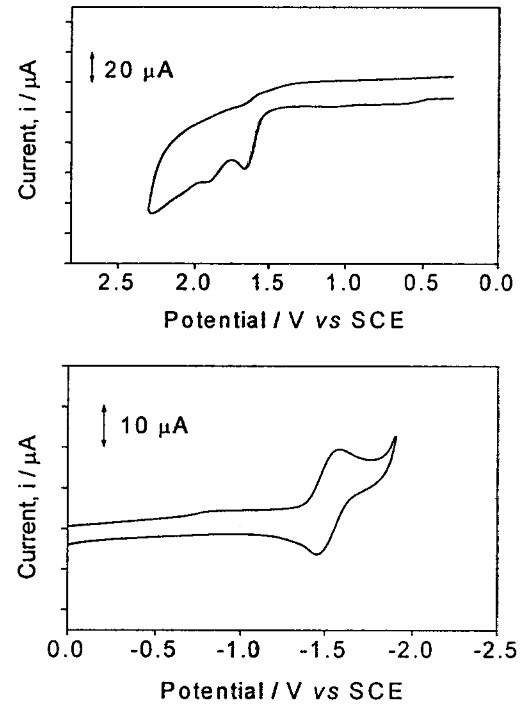

Figure 6. Cyclic voltammograms showing (a) the oxidation (scan rate, 100 mV s^{-1}) and (b) reduction (scan rate, 100 mV s^{-1}) of [(bpy)Zn_2-(SC_6H_5)(μ-SC_6H_5)(μ-OAc)$_2$] (**1**) in dichloromethane (0.1 mol dm^{-3} $^{n}Bu_4NPF_6$).

To further understand and establish the presence of various conformations of **3** at low temperature, signal assignment in the two-dimensional ^{1}H NMR spectra was achieved by means of 2D COSY and EXSY experiments[12b−c,16] at 223 K in CD_2Cl_2 as shown in Figure 5. In the 2D COSY spectrum, coupling between vicinal aryl protons among the same species was observed, while in the 2D EXSY spectrum, the pattern of the cross-peaks observed that was not found in COSY spectrum is characteristic for the mechanism of the exchange process of thiolate ligands and possibly the different orientation of the lone pair electrons on neighboring sulfur atom[15] which further supported the presence of various different conformations of **3** in solution at low temperature. The various possible conformations of the complex were proposed and shown in Scheme 1.

Electrochemical Properties. The electrochemical properties of complexes **1**−**5** have been investigated by cyclic voltammetry. The electrochemical data for **1**−**5** in dichloromethane are summarized in Table 3. Figure 6 depicts the cyclic voltammograms of **1**. The cyclic voltammograms of **1**−**5** display two irreversible oxidation waves (+1.30 to +1.99 V vs SCE) and one quasi-reversible reduction couple (−1.52 to −1.62 V vs SCE). In view of the redox inactive nature of Zn(II) and the observation that the oxidation waves appear to vary with the nature of the thiophenolate ligands, the two oxidation waves are tentatively assigned as the thiophenolate ligand-centered oxidations. It is likely that the less positive oxidation wave of the two at +1.30 to +1.7 V vs SCE is due to the oxidation at

(15) (a) Knotter, D. M.; Blasse, G.; van Vliet, J. P. M.; van Koten, G. *Inorg. Chem.* **1992**, *31*, 2196. (b) Iwasaki, F.; Yoshida, S.; Kakuma, S.; Watanabe, T.; Yasui, M. *J. Mol. Sci.* **1995**, *352*, 203.
(16) Günther, H. *NMR Spectroscopy: Basic Principles, Concepts, and Applications in Chemistry*, 2nd ed.; John Wiley & Sons: Germany, 1994.

the terminal thiophenolate ligand, while the more positive one at ca. +1.6 to +2.0 V is that at the less electron rich bridging thiophenolate ligand. The least positive potential for the oxidation of **4** (+1.44 and +1.73 V vs SCE) than that of **1**, **2**, and **3** is in accordance with the presence of the more electron rich methoxy group substituted on the thiophenolate, resulting in an increased ease of oxidation on the thiophenolate ligand. The potentials for the oxidation of **1** and **5** are similar as both complexes bear the same thiophenolate ligand. Similar to the observation in UV/vis and emission data, the potentials for the oxidation of **2** are unexpectedly found to be much less positive relative to **1**, suggestive of a domination of the resonance effect of lone pairs on F atom donating to the thiophenolate over the negative indicative effect of F, giving rise to an anomalous increase in the ease of oxidation of 4-fluorothiophenolate in **2** relative to that of **1**. On the other hand, the quasi-reversible reduction couple is likely to originate from a diimine ligand-centered reduction, as such potentials are very similar for complexes **1**−**4**, which have the same bpy ligand. The more negative reduction potential observed in **5** (−1.62 V vs SCE) than that of **1** (−1.52 V vs SCE) is in agreement with the reduced ease of reduction of $^{t}Bu_2$bpy as a result of its higher π^* orbital energy. The observation of thiophenolate-centered oxidation and diimine-centered reduction processes further establishes the LLCT nature of the lowest energy electronic transition.

Acknowledgment. V.W.-W.Y. acknowledges financial support from the Research Grants Council and The University of Hong Kong. Y.-L.P. acknowledges the receipt of a postgraduate studentship, administered by The University of Hong Kong. Helpful discussions with Dr. H. Z. Sun on the NMR measurements are gratefully acknowledged.

Supporting Information Available: Tables giving atomic coordinates, anisotropic displacement parameters, bond lengths and bond angles for complex **3**. A CIF file. This material is available free of charge via the Internet at http://pubs.acs.org.

IC000688G